International Journal of Bifurcation and Chaos, Vol. 17, No. 5 (2007) 1713–1719

A CMOS REACTION–DIFFUSION DEVICE USING MINORITY-CARRIER DIFFUSION IN SEMICONDUCTORS

MOTOYOSHI TAKAHASHI, TETSUYA ASAI*, TETSUYA HIROSE and YOSHIHITO AMEMIYA
Graduate School of Information Science and Technology, Hokkaido University, Kita 14, Nishi 9, Sapporo 060-0814, Japan
**asai@sapiens-ei.eng.hokudai.ac.jp*

Received March 21, 2006; Revised May 5, 2006

We propose a CMOS device that is analogous to the reaction–diffusion system, a chemical complex system that produces various dynamic phenomena in the natural world. This electrical reaction–diffusion device consists of an array of *pn* junctions that are operated by CMOS reaction circuits and interact with each other through minority-carrier diffusion. Computer simulations reveal that the device can produce animated spatiotemporal carrier concentration patterns, e.g. expanding circular patterns and rotating spiral patterns that correspond to the dissipative structures produced by chemical reaction–diffusion systems.

Keywords: Reaction–diffusion systems; analog integrated circuits; minority-carrier transport.

1. Introduction

A promising area of research in microelectronics is the development of electrical devices that imitate the behavior of reaction–diffusion systems (RD systems), which are chemical complex systems that produce dynamic, self-organizing natural phenomena. In this paper we propose a silicon RD device that consists of CMOS circuits combined with minority-carrier diffusion. Creating an electrical analog of RD systems would enables us to imitate some of natural phenomena on silicon LSI chips to develop nature-based information processing systems.

Semiconductor RD computing LSIs (chips) implementing RD dynamics have been proposed in the literature [Adamatzky *et al.*, 2005]. These chips were mostly designed by digital, analog, or mixed-signal complementally-metal-oxide-semiconductor (CMOS) circuits of cellular neural networks (CNNs) or cellular automata (CA). Electrical cell circuits were designed to implement several CA and CNN models of RD systems [Adamatzky *et al.*, 2004; Asai *et al.*, 2002; Matsubara *et al.*, 2004; Rekeczky *et al.*, 2003; Shi & Luo, 2004], as well as fundamental reaction–diffusion equations [Asai *et al.*, 2005; Daikoku *et al.*, 2002; Karahaliloglu & Balkir, 2005; Serrano & Linares, 2003]. Each cell is arranged on a 2D square or hexagonal grid and is connected with adjacent cells through coupling devices that transmit a cell's state to its neighboring cells, as in conventional CAs. For instance, an analog-digital hybrid RD chip [Asai *et al.*, 2002] was designed for emulating a conventional CA model for Belousov–Zhabotinsky (BZ) reactions [Gerhardt *et al.*, 1990]. A full-digital RD processor [Matsubara *et al.*, 2004] was also designed on the basis of a multiple-valued CA model, called *excitable lattices* [Adamatzky, 2001]. An analog cell circuit was also designed to be equivalent to spatial-discrete Turing RD systems [Daikoku *et al.*, 2002]. A full-analog RD chip that

emulates BZ reactions has also been designed and fabricated [Asai *et al.*, 2005].

Blueprints of non-CMOS RD chips have been designed; i.e. a single-electron RD device [Oya *et al.*, 2005]. The authors previously proposed a RD device based on minority-carrier transport in semiconductor devices [Asai *et al.*, 2004]. The point of our idea was to simulate chemical diffusion with minority-carrier diffusion in semiconductors and autocatalystic chemical reactions with carrier multiplication in *pnpn* negative resistance diodes. In this paper, we propose an improved device that uses CMOS feedback circuits instead of *pnpn* diodes. Using CMOS circuits enables us to simulate a variety of autocatalystic reactions and opens up a variety of application fields for RD devices.

2. Electrical RD Device Consisting of a *p*-Cell Array on an *n*-Type Substrate

A reaction–diffusion system can be considered an aggregate of chemical-reaction cells, each of which represents a local chemical reaction. Each cell interacts with its neighbors through a nonlocal chemical diffusion. To imitate such systems, we propose a cell array device, or a two-dimensional electrical RD device, as shown in Fig. 1. It consists of p-type islands, or p cells, in a regular arrangement on an n-type substrate, with each cell connected to a CMOS feedback circuit that simulates autocatalystic reactions. This CMOS circuit is called a reaction circuit.

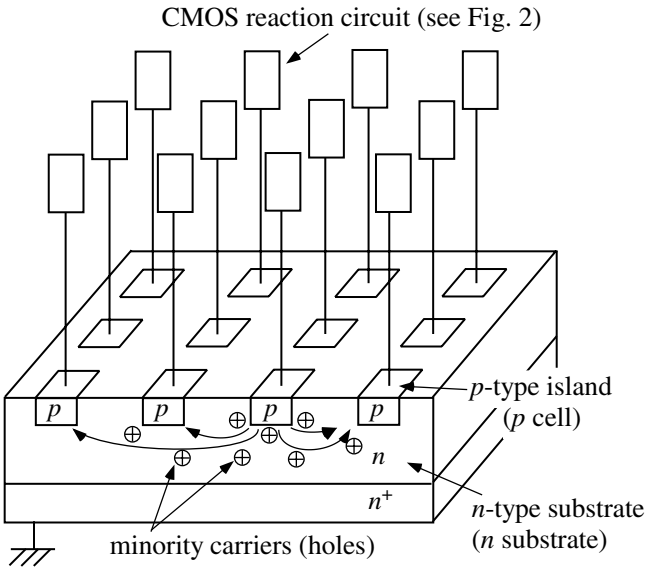

Fig. 1. RD device consisting of p-cell array on n substrate, with each cell connected to CMOS reaction circuit.

In operation, the n substrate is grounded. If a p cell has a positive, it injects minority carriers (holes) into the substrate. The injected holes spread and travel by diffusion through the substrate until they reach the neighboring p cells and raise the cell. Through this diffusion of minority carriers, the p cells interact and correlate with one another.

To implement RD dynamics such as spatiotemporal pattern formation, the p cell has to exhibit excitatory behavior as follows:

(1) The cell is static in its normal (stationary) state and does not inject any minority carriers into the substrate;
(2) Once the cell receives a few minority carriers from the neighboring cells, it becomes excited and injects many minority carriers into the substrate (excited state);
(3) The excited cell cools down quickly and gradually returns to a stationary state. It cannot be excited again during this refractory state.

To obtain this excitatory behavior, we drive the p cells with CMOS reaction circuits, as shown in the next section.

3. Driving *p* Cells with CMOS Reaction Circuits

The CMOS reaction circuits that activate the p cells are illustrated in Fig. 2. They consist of four M1–M4 transistors and a capacitor C, biased with a positive voltage $V_{\rm dd}$. The M1 gate, or node 1, is connected to the p cell in the cell array. Transistors M3 and M4 are biased by a current source I_0 and transistor M5.

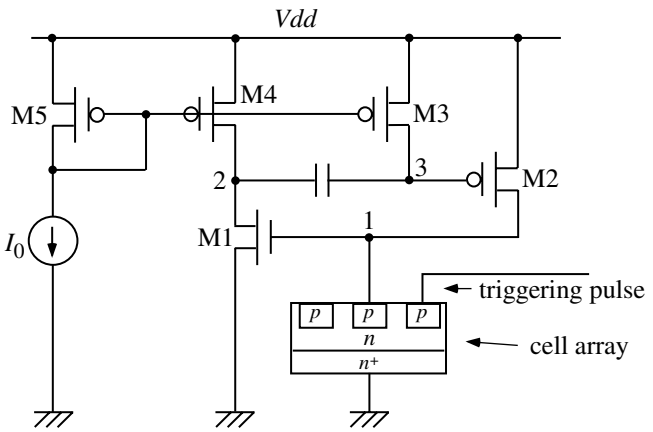

Fig. 2. CMOS reaction circuit together with p-cell array to operate a p cell.

They supply a current to nodes 2 and 3. Transistors M1 and M2 and capacitor C form a monostable feedback loop. The point in constructing this reaction circuit is to set the M1 threshold voltage lower than the forward voltage drop of the cell-substrate *pn* junction. The circuits with the p cell array can be made on a chip by means of SOI (silicon-on-insulator) process technology. The circuit operation is as follows:

- *Stationary state*
  Without minority carriers around the p cell, the voltage of node 1 is zero. So M1 is in the off position. Therefore, the voltages of nodes 2 and 3 are $V_{\rm dd}$, and M2 is off. No minority carrier is injected from the cell into the substrate.
- *Excited state*
  Suppose minority carriers (holes) flow into the cell from neighboring cells. Then the voltage of the cell (node 1) rises and exceeds the threshold voltage of M1. This excites the circuit as follows: M1 is turned on, → the voltage of node 2 falls to about 0, → the voltage of capacitively coupled node 3 also falls to about 0, → M2 is turned on, → the current flows through the cell-substrate *pn* junction. Consequently, the cell injects many minority carriers into the substrate.
- *Refractory state*
  The voltage of node 3 quickly returns to $V_{\rm dd}$ because of the current through M3. This turns M2 off, so the cell ceases its minority-carrier injection. Then the voltage of node 2 gradually returns to $V_{\rm dd}$ because of the current through M4. The circuit cannot be excited again before the voltage of node 2 exceeds the threshold voltage of M2. This is so because the voltage of node 3 cannot be sufficiently decreased to turn on M2 even if the voltage of node 2 falls to 0. The circuit returns to the stationary state when the voltage of node 3 rises to $V_{\rm dd}$. The duration of the excited and refractory states can be controlled by adjusting the currents through M3 and M4.

4. Operation of the Reaction Circuit Combined with *p* Cell

Figure 3 shows the computer-simulated (SPICE) operation of the reaction circuit. For MOS FETs in the proposed circuit, we used a 1.5-μm CMOS parameters provided by MOSIS (Vendor: AMIS). To simulate the carrier transport between two cells, we considered the cells and the substrate from a lateral *pnp* bipolar transistor. To excite the circuit, we applied three current pulses to the p cell adjacent to the cell connected to the circuit (see Fig. 2). The first two pulses were applied at short time intervals and the third pulse after a long wait [Fig. 3(a)]. Triggered by the first pulse, the circuit excited and lowered the voltages of node 2 and 3 [Fig. 3(b)] and turned on M2, to pass a current through the cell-substrate *pn* junction [Fig. 3(c)]. However, the circuit was not excited by the second pulse because it was in a refractory state — i.e. it had not yet recovered the voltage of node 2. After a short time, the

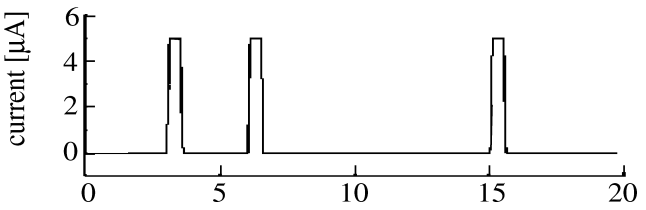

(a) Triggering current pulses

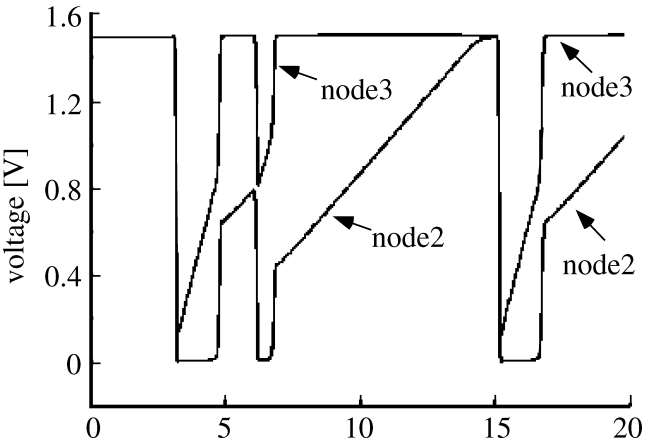

(b) Node voltages

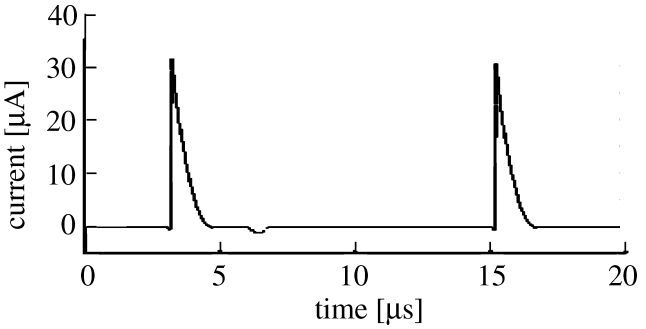

(c) Cell-substrate junction current

Fig. 3. Reaction circuit operation; (a) triggering current pulses applied to an adjacent cell (see Fig. 2), (b) voltage waveforms on nodes 2 and 3, and (c) forward current through the cell-substrate *pn* junction, simulated with a set of AMIS 1.5-μm CMOS parameters (MOSIS).

circuit recovered the node voltage and returned to the stationary state, before being reexcited by a third pulse.

Excitation can be transmitted along the p cells. This is illustrated in Fig. 4 with simulated results for a one-dimensional array of 100 cells connected to reaction circuits. Minority carriers were injected at the leftmost cell with a triggering pulse [Fig. 4(a)]. Excitation started at the adjacent cell and traveled to the right along the cell array. In other words, the minority-carrier wave traveled rightward in the substrate. This is shown in Fig. 4(b); the concentration of minority carriers beneath each cell was calculated from the cell voltage.

Figure 5 shows a collision between two minority-carrier waves. In this example, a 100-cell array was excited at both ends at $t = 1$ μs, and two waves were generated to run toward each other. In the middle of the cell array, the waves collided head-on with each other in the middle of the cell array and then vanished without leaving a trace.

In our proposed RD device, the minority-carrier concentration in the substrate surrounding each cell changes temporally as the cells interact with each other. Consequently, a two-dimensional spatiotemporal pattern of carrier concentration is produced in the RD device. Since this carrier-concentration pattern corresponds to the dissipative structure in chemical RD systems, it can be called an electrical dissipative structure. A variety of spatiotemporal patterns are produced from different set of system parameters. Here we show three examples, simulated with a sample set of parameter values. The following figures show the results for RD devices consisting of 21 × 21 cells with 441 reaction circuits. A gray scale represents the carrier concentration around each cell: light shading means a high concentration, and dark shading means a low concentration.

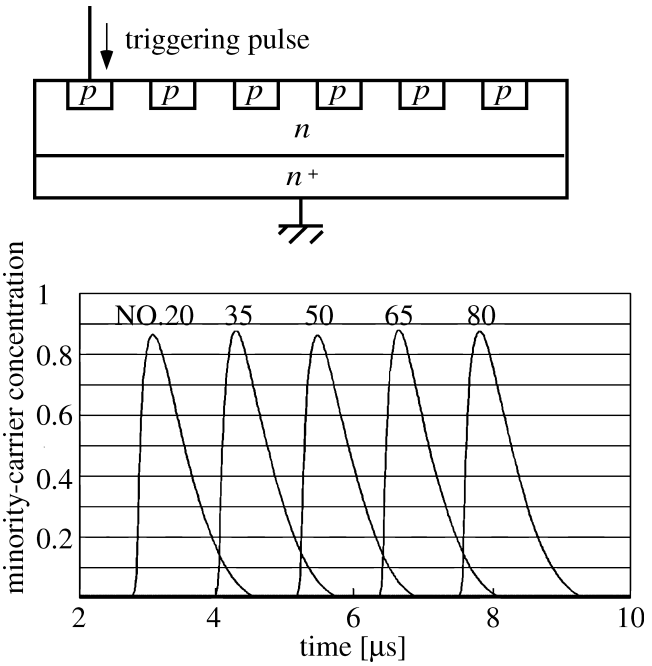

Fig. 4. Transmission of an excited minority-carrier wave along a 100-cell array; (a) one-dimensional p-cell array, and (b) minority-carrier concentration beneath each cell. The number for each waveform indicates the number of the corresponding cell: the leftmost cell is No. 1 and the rightmost is No. 100. The minority-carrier concentration is normalized with respect to $10^{11} \times p_0$, where p_0 is the equilibrium hole concentration in the n substrate.

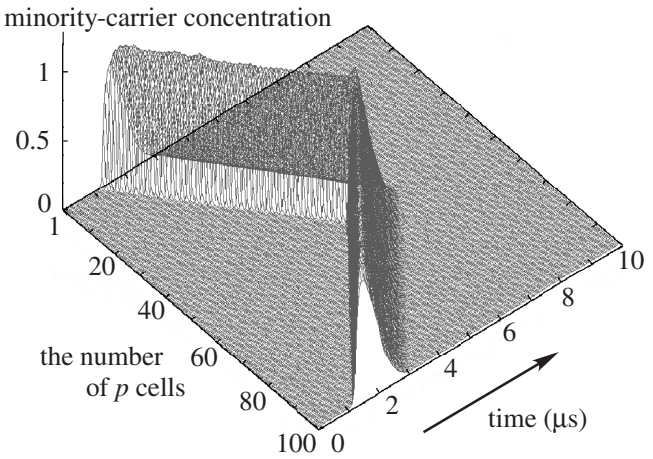

Fig. 5. Collision between two minority-carrier waves on a one-dimensional p-cell array. Two waves started from both ends of the array and collided in the middle. The minority-carrier concentration is normalized with respect to $10^{11} \times p_0$, where p_0 is the equilibrium hole concentration in the n substrate.

- *Expanding circular pattern*
  The RD device is in a uniform, stable state as it stands. Once a triggering pulse is applied to a cell in the device, the minority-carrier excitation wave starts at the cell and propagates in all directions to form an expanding circular pattern. This is shown in Fig. 6. The front of the waves is the region where cells are just excited and, therefore, where the minority-carrier concentration is the highest, as indicated by the light shading. At the back of the wave, the minority-carrier concentration gradually decreases to its thermal equilibrium value, as indicated by the dark shading [see Fig. 6(c)].

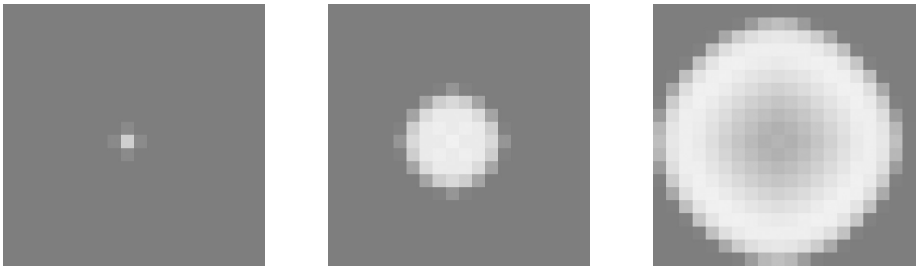

(a) time = 0.2 μs (b) 0.5 μs (c)1 μs

Fig. 6. Expanding circular pattern. Snapshots for three time steps. The center cell was excited at $t = 0$.

- *Collision between two circular patterns*
  Figure 7 shows a collision between two waves. In this example, the two diagonally opposed in the RD device were excited at $t = 0$. Two minority-carrier excitation wave started at the cells and propagated to form expanding circular patterns [Figs. 7(a)–7(c)]. The two circular waves collided in the center and vanished without leaving a trace [Figs. 7(d)–7(f)].
- *Rotating spiral pattern*
  Figure 8 shows a rotating spiral pattern. This pattern appears when an expanding circular wave is chipped by an external disturbance, thereby causing the endpoint to appear in front of the wave. With this endpoint acting as the center, the wave begins to curl itself to form a rotating spiral pattern. In this example, a trigger was applied to the middle cell on the left of the RD system at $t = 0$. When the excitation wave started at the cell and expanded slightly, the lower half of the wave was chipped by resetting the cell voltage 0 [Figs. 8(a)–8(c)]. After that, the RD device was left to operate freely, and a rotating spiral pattern by carrier concentration was automatically generated as can be seen in Figs. 8(d)–8(f).

These results indicate the expected operations of the RD device. The next challenge is to develop RD devices with a more microscopic process because a large number of reaction cells must be

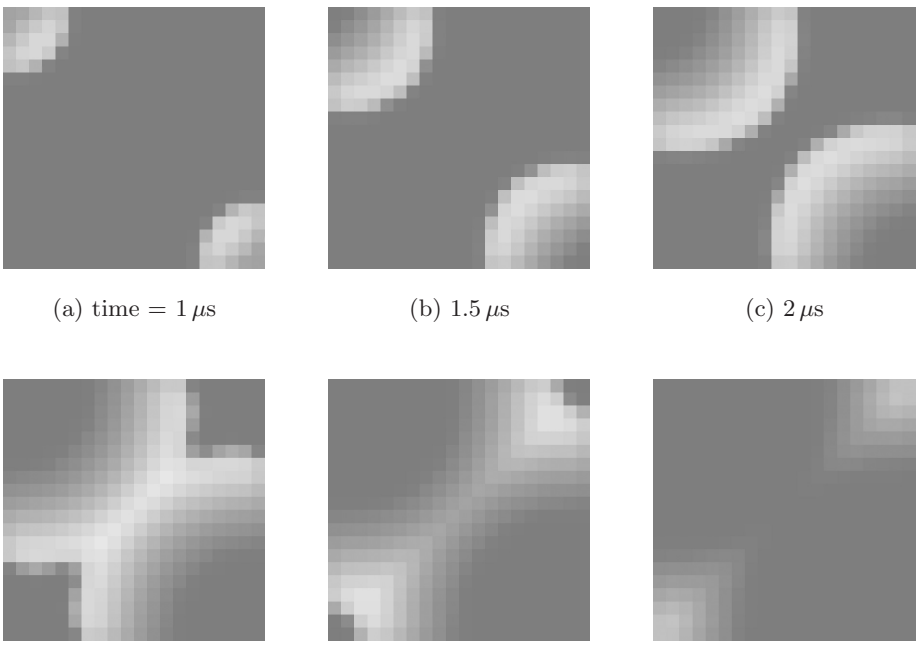

(a) time = 1 μs (b) 1.5 μs (c) 2 μs

(d) 2.5 μs (e) 3 μs (f) 3.5 μs

Fig. 7. Collision between two circular waves. Snapshots for six time steps. Two minority-carrier waves started at diagonal corners, expanded to form circular patterns, and collided with each other in the center.

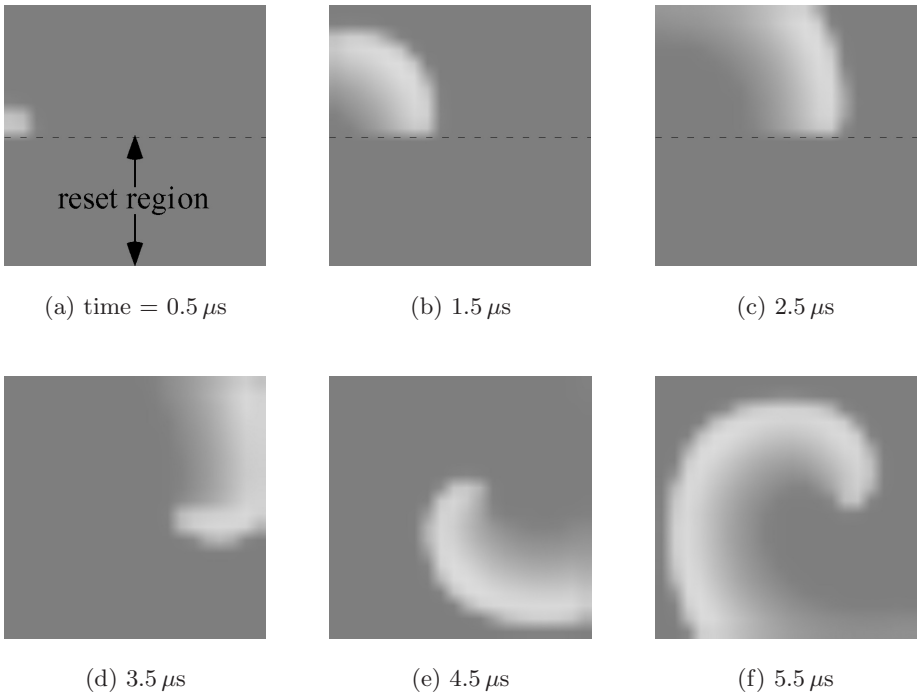

(a) time = 0.5 μs (b) 1.5 μs (c) 2.5 μs

(d) 3.5 μs (e) 4.5 μs (f) 5.5 μs

Fig. 8. Rotating spiral pattern. Snapshots for six time steps. A circular wave started in the middle on the left edge. It was chipped by resetting (a)–(c) and transformed into a spreading spiral pattern (d)–(f).

implemented on a chip to observe complex (BZ-like) patterns. Furthermore, at this stage, each reaction cell should have optical sensors for parallel inputs. In fact, the optical input of data-information was already used at the beginning of RD research [Kuhnert *et al.*, 1989]. This was proven to be particularly important in experiments on image processing in BZ-medium-based computing devices.

5. Summary

Silicon devices that imitate the autocatalytic and dissipative phenomena of reaction–diffusion (RD) systems were introduced. This novel silicon device imitates auto-catalytic and dissipative phenomena of the chemical RD systems, however comparing to real chemical medium the semi-conductor analog of RD computers, functions much faster. We studied operational characteristics of the RD silicon devices and demonstrate feasibility of the approach on several computational tasks. Our results indicate that the proposed RD device will be a useful tool for developing novel hardware architectures based on RD principles of information processing.

Acknowledgments

The authors wish to thank Professor Andrew Adamatzky of the University of the West of England for most valuable discussions and suggestions during the research. This study was partly supported by Industrial Technology Research Grant Program in '04 from New Energy and Industrial Technology Development Organization (NEDO) of Japan, and a Grant-in-Aid for Young Scientists [(B)17760269] from the Ministry of Education, Culture Sports, Science and Technology (MEXT) of Japan.

References

Adamatzky, A. [2001] *Computing in Nonlinear Media and Automata Collectives* (IOP Publishing, Bristol).

Adamatzky, A., Arena, P., Basile, A., Carmona-Galán, R., De Lacy Costello, B., Fortuna, L., Frasca, M. & Rodríguez-Vázquez, A. [2004] "Reaction–diffusion navigation robot control: From chemical to VLSI analogic processors," *IEEE Trans. Circuit Syst.-I* **51**, 926–938.

Adamatzky, A., De Lacy Costello, B. & Asai T. [2005] *Reaction–Diffusion Computers* (Elsevier, London).

Asai, T., Nishimiya, Y. & Amemiya, Y. [2002] "A CMOS reaction–diffusion circuit based on cellular-automaton processing emulating the Belousov–Zhabotinsky reaction," *IEICE Trans. Fund.* **E85-A**, 2093–2096.

Asai, T., Adamatzky, A. & Amemiya, Y. [2004] "Towards reaction–diffusion computing devices based on minority-carrier transport in semiconductors," *Chaos Solit. Fract.* **20**, 863–876.

Asai, T., Kanazawa, Y., Hirose, T. & Amemiya, Y. [2005] "Analog reaction–diffusion chip imitating the Belousov–Zhabotinsky reaction with hardware oregonator model," *Int. J. Unconvent. Comput.* **1**, 123–147.

Bonaiuto, V., Maffucci, A., Miano, G., Salerno, M., Sargeni, F., Serra, P. & Visone, C. [2001] "Hardware implementation of a CNN for analog simulation of reaction–diffusion equations," in *Proc. IEEE Int. Conf. Circuits Syst.* **3**, 485–488.

Daikoku, T., Asai, T., and Amemiya, Y. [2002] "An analog CMOS circuit implementing Turing's reaction–diffusion model," in *Proc. Int. Symp. Nonlinear Theory and its Applications*, pp. 809–812.

Gerhardt, M., Schuster, H. & Tyson, J. J. [1990] "A cellular automaton model of excitable media," *Physica D* **46**, 392–415.

Karahaliloglu, K. & Balkir, S. [2005] "Bio-inspired compact cell circuit for reaction–diffusion systems," *IEEE Trans. Circuit Syst.-II* **52**, 558–562.

Kuhnert, L., Agladze, K. L. & Krinsky, V. I. [1989] "Image processing using light-sensitive chemical waves," *Nature* **337**, 244–247.

Matsubara, Y., Asai, T., Hirose, T. & Amemiya, Y. [2004] "Reaction–diffusion chip implementing excitable lattices with multiple-valued cellular automata," *IEICE Electron. Expr.* **1**, 248–252.

Oya, T., Asai, T., Fukui, T. & Amemiya Y. [2005] "Reaction–diffusion systems consisting of single-electron circuits," *Int. J. Unconvent. Comput.* **1**, 177–194.

Rekeczky, C., Roska, T., Carmona, R., Jiménez-Garrido, F. & Rodríguez-Vázquez, A. [2003] "Exploration of spatial-temporal dynamic phenomena in a 32 × 32-cell stored program two-layer CNN universal machine chip prototype," *J. Circuits Syst. Comput.* **12**, 691–710.

Serrano-Gotarredona, T. & Linares-Barranco, B. [2003] "Log-domain implementation of complex dynamics reaction–diffusion neural networks," *IEEE Trans. Neural Networks* **14**, 1337–1355.

Shi, B. E. & Luo, B. T. [2004] "Spatial pattern formation via reaction–diffusion dynamics in 32 × 32 × 4 CNN chip," *IEEE Trans. Circuit Syst.-I* **51**, 939–947.